Electronic Supplementary Information (ESI)

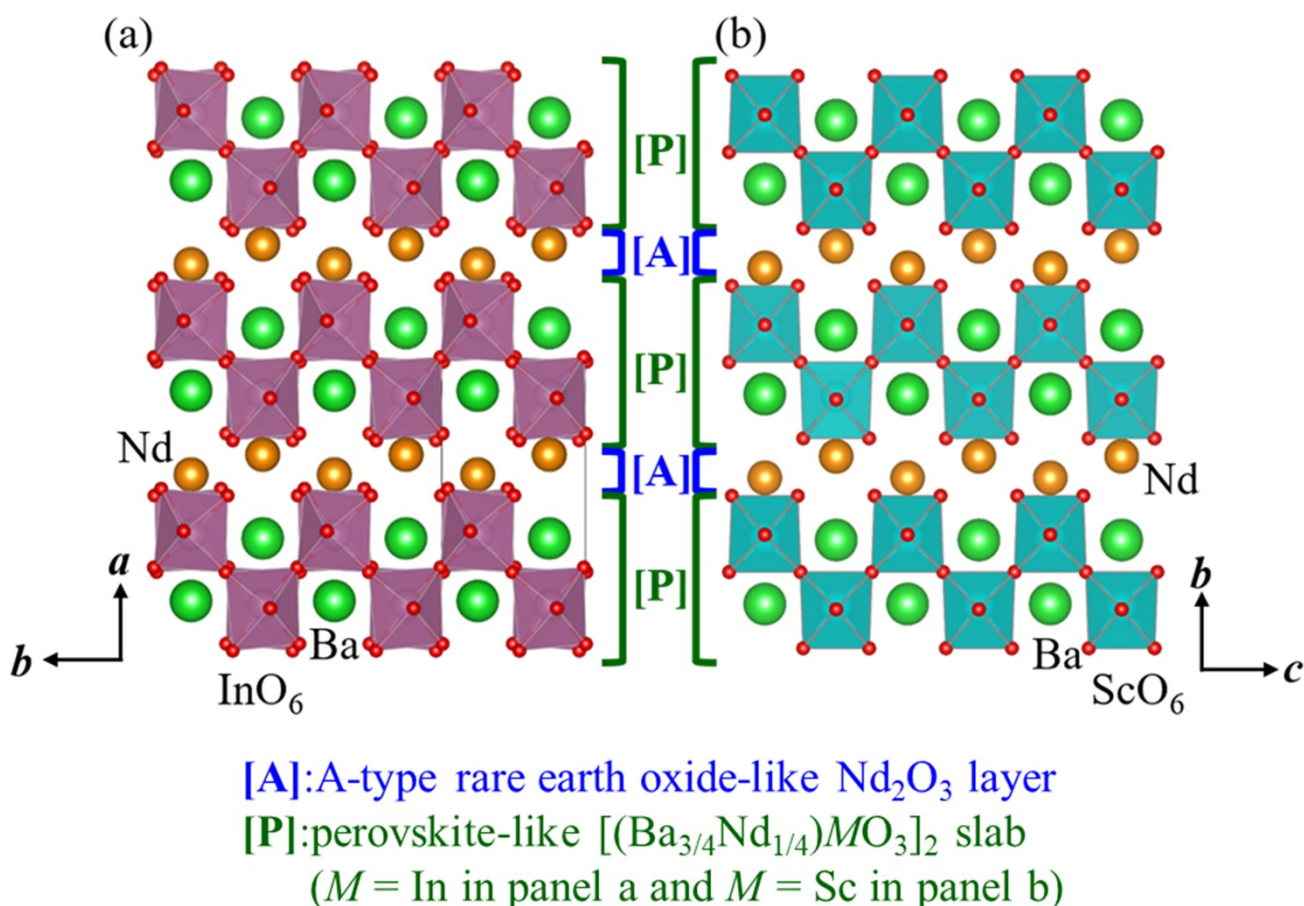# High-temperature proton conductors based on the (110) layered perovskite BaNdScO$_4$

Masahiro Shiraiwa, Takafusa Kido, Kotaro Fujii, Masatomo Yashima[*]

Department of Chemistry, School of Science, Tokyo Institute of Technology, 2−12−1−W4−17,

O−okayama, Meguro−ku, Tokyo 152−8551, Japan

* Corresponding author

(A)   Crystal structures of BaNdInO$_4$ and BaNdScO$_4$

[A]:A-type rare earth oxide-like Nd$_2$O$_3$ layer
[P]:perovskite-like [(Ba$_{3/4}$Nd$_{1/4}$)MO$_3$]$_2$ slab
(M = In in panel a and M = Sc in panel b)

Figure S1. Crystal structures of (a) BaNdInO$_4$ (*Chem. Mater.*, 2014, **26**, 2488–2491) and (b) BaNdScO$_4$ (*Chem. Commun*, 2016, **52**, 10980–10983). Red sphere denotes an oxygen atom. (a) BaNdInO$_4$ with the monoclinic $P2_1/c$ BaNdInO$_4$-type structure. (b) BaNdScO$_4$ with the orthorhombic *Cmcm* BaNdInO$_4$-type structure.

(B) XRD patterns of BaNd$_{1-x}$A$_x$ScO$_{4-x/2}$
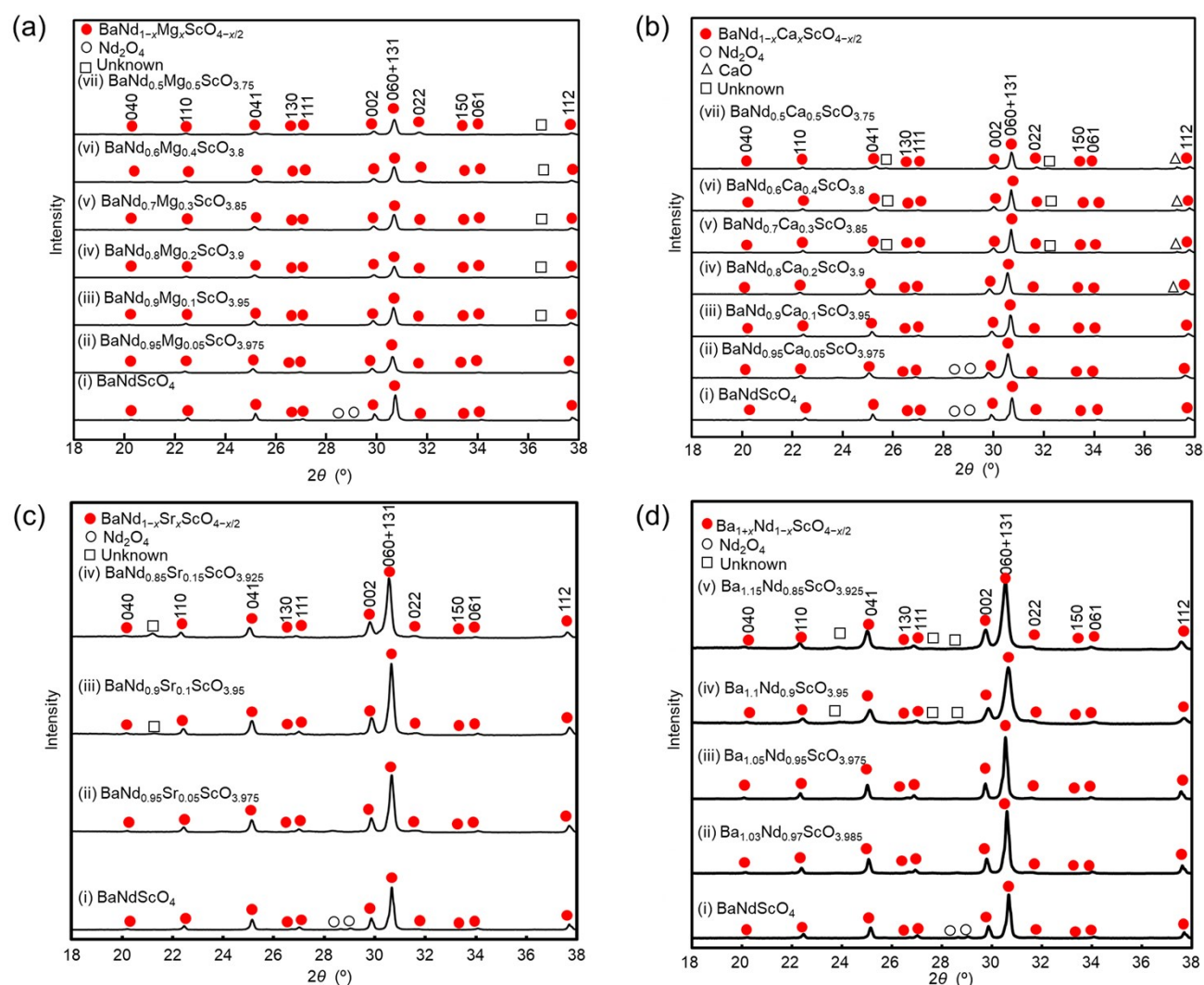
Figure S2. Cu $K\alpha$ X-ray powder diffraction patterns of BaNd$_{1-x}$A$_x$ScO$_{4-x/2}$ at room temperature. (a) x = (i) 0.0, (ii) 0.05, (iii) 0.1, (iv) 0.2, (v) 0.3, (vi) 0.4 and (vii) 0.5 for A = Mg. (b) x = (i) 0.0, (ii) 0.05, (iii) 0.1, (iv) 0.2, (v) 0.3, (vi) 0.4 and (vii) 0.5 for A = Ca. (c) x = (i) 0.0, (ii) 0.05, (iii) 0.1 and (iv) 0.15 for A = Sr. (d) x = (i) 0.0, (ii) 0.03, (iii) 0.05, (iv) 0.1 and (v) 0.15 for A = Ba.

(C) Lattice parameters of BaNd$_{1-x}$Ca$_x$ScO$_{4-x/2}$
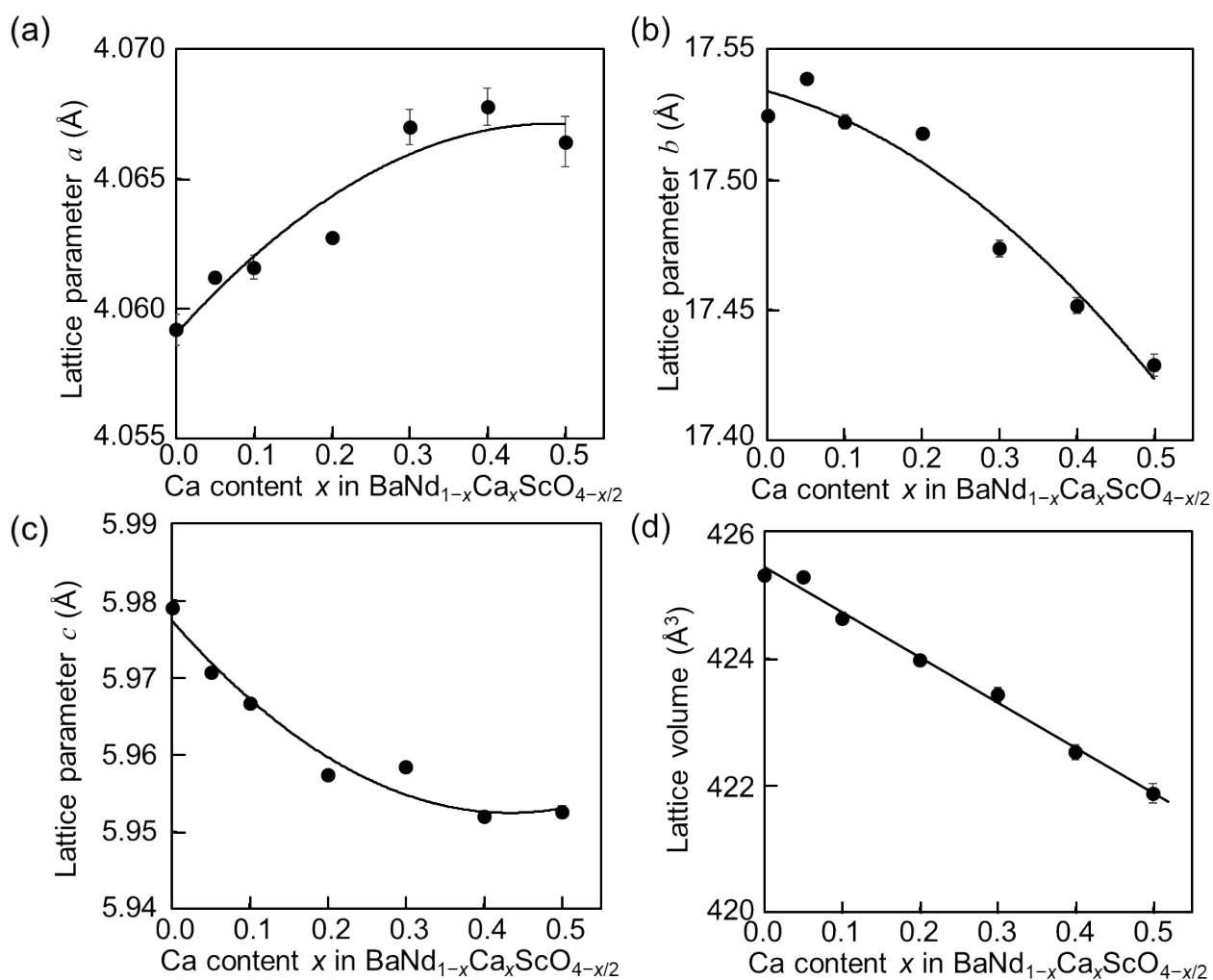
Figure S3. Variation of lattice parameters (a) a, (b) b and (c) c and (d) lattice volume of orthorhombic *Cmcm* BaNd$_{1-x}$Ca$_x$ScO$_{4-x/2}$ with Ca content x (x = 0.0, 0.05, 0.1, 0.2, 0.3, 0.4, 0.5) at 23 °C.

Table S1. Lattice parameters and lattice volume of orthorhombic *Cmcm* phase in $BaNd_{1-x}Ca_xScO_{4-x/2}$ powders (x = 0.0, 0.05, 0.1, 0.2, 0.3, 0.4 and 0.5) versus Ca content x at 23 °C. These parameters of $BaNd_{1-x}Ca_xScO_{4-x/2}$ (x = 0.0, 0.05, 0.1, 0.2, 0.3, 0.4 and 0.5) were determined by the Le Bail analyses using the Cu $K\alpha$ X-ray powder diffraction data measured at 23 °C.

x	a (Å)	b (Å)	c (Å)	Lattice volume (Å^3)
0	4.0592(7)	17.524(3)	5.9791(5)	425.32(10)
0.05	4.0612(3)	17.5388(10)	5.9708(4)	425.29(4)
0.1	4.0616(5)	17.522(3)	5.9667(7)	424.63(10)
0.2	4.06274(15)	17.5177(7)	5.9574(2)	423.98(3)
0.3	4.0670(7)	17.474(4)	5.9584(7)	423.43(12)
0.4	4.06777(8)	17.452(3)	5.9520(6)	422.52(12)
0.5	4.06643(10)	17.429(5)	5.9526(8)	421.88(16)

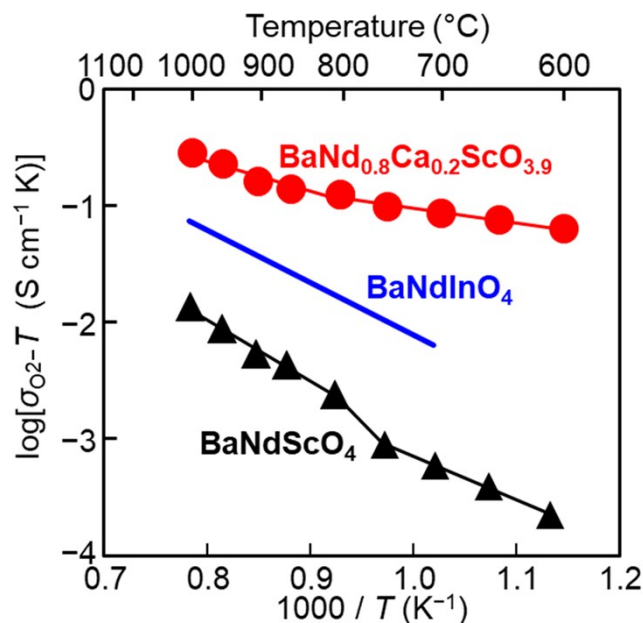## (D) UV−Vis diffuse reflectance spectra
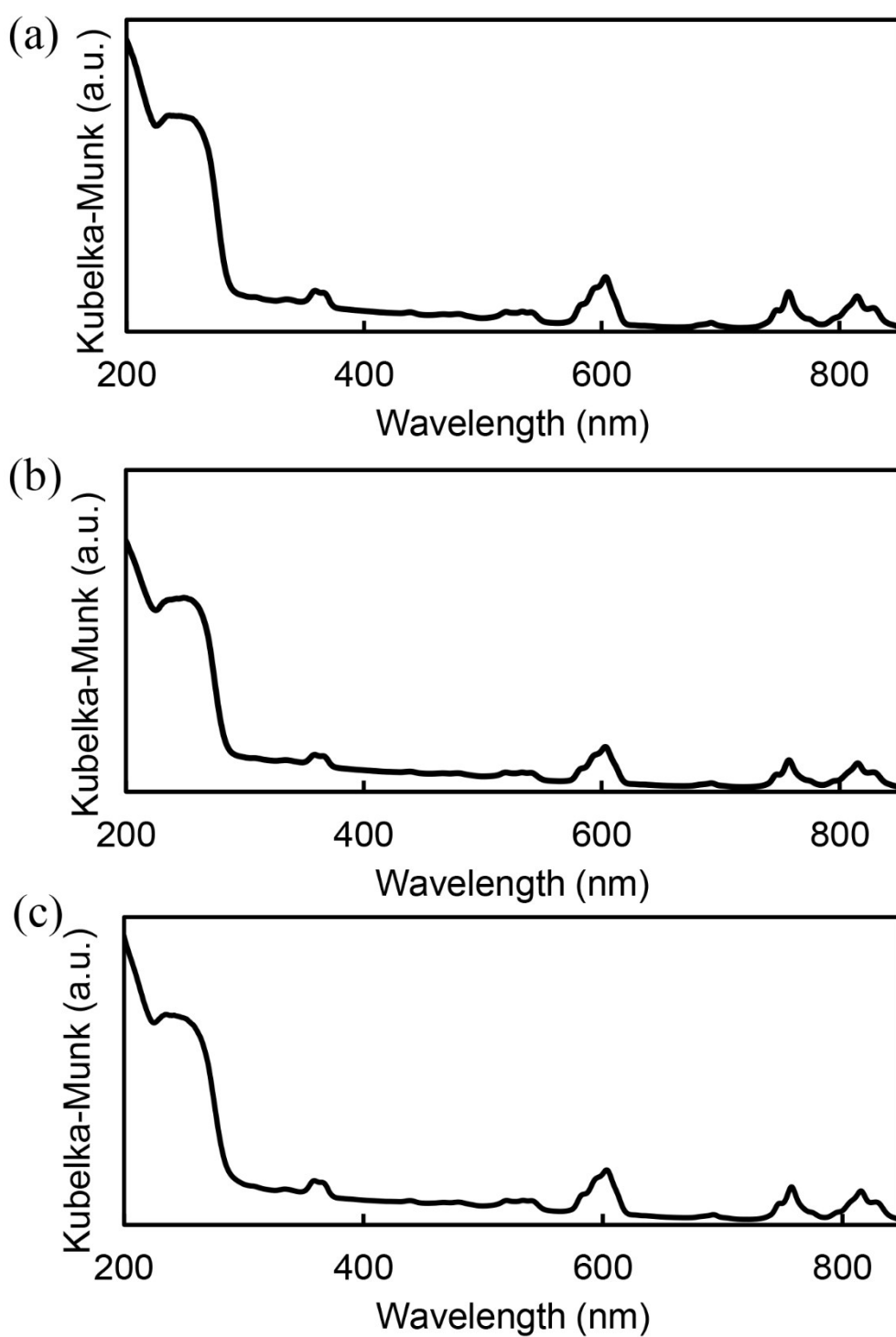

Figure S4. UV−Vis diffuse reflectance spectra of (a) $BaNdScO_4$, (b) $BaNd_{0.9}Ca_{0.1}ScO_{3.95}$ and (c) $BaNd_{0.8}Ca_{0.2}ScO_{3.9}$.

(E) Arrhenius plots of oxide-ion conductivities

Figure S5. Arrhenius plots of oxide-ion conductivities $\sigma_{o^{2-}}$ of BaNScO$_4$ (black), BaNd$_{0.8}$Ca$_{0.2}$ScO$_{3.9}$ (red) and BaNdInO$_4$ (blue). The activation energies of $\sigma_{o^{2-}}$ of BaNdScO$_4$ were 0.92(12) eV in the temperature range of 600-800 °C and 1.04(5) eV above 800 °C. These values are higher than those of BaNd$_{0.8}$Ca$_{0.2}$ScO$_{3.9}$ (0.25(2) eV in the temperature range of 600-800 °C and 0.51(8) eV above 800 °C) and seem to be higher than that of BaNdInO$_4$ in the temperature range of 700-1000 °C (0.89(4) eV) (*J. Electrochem. Soc.*, 2017, **164**, F1392-F1399). Higher activation energy for oxide-ion conductivity of BaNdScO$_4$ (E_a = 1.04 eV above 800°C) than that of BaNdInO$_4$ (E_a = 0.89 eV) is consistent with the higher bond-valence-based energy (BVE) barrier for oxide-ion migration of BaNdScO$_4$ (1.97 eV) than that of BaNdInO$_4$ (0.77 eV), which is attributable to the smaller bottleneck size (critical radius) for oxide-ion migration of BaNdScO$_4$ 1.0377(7) Å than that of BaNdInO$_4$ 1.0666(2) Å (*Chem. Mater.*, 2014, **26**, 2488–2491).

(F) Proton transport number
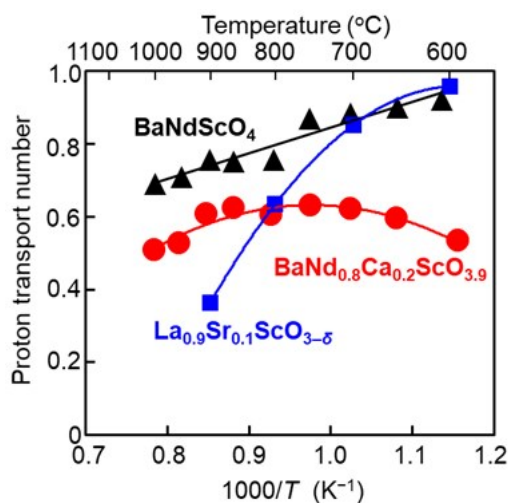
Figure S6. Proton transport numbers of BaNdScO$_4$ (this work), BaNd$_{0.8}$Ca$_{0.2}$ScO$_{3.9}$ (this work) and La$_{0.9}$Sr$_{0.1}$ScO$_{3-\delta}$ (*Solid State Ionics*, 2017, **306**, 126–136).

Table S2. Proton transport numbers of BaNdScO$_4$ (this work), BaNd$_{0.8}$Ca$_{0.2}$ScO$_{3.9}$ (this work) and La$_{0.9}$Sr$_{0.1}$ScO$_{3-\delta}$ (*Solid State Ionics*, 2017, **306**, 126–136). The proton transport number of BaNdScO$_4$ is comparable with that of La$_{0.9}$Sr$_{0.1}$ScO$_{3-\delta}$ at 600 and 700 ˚C, while the proton transport number of BaNdScO$_4$ is higher than that of La$_{0.9}$Sr$_{0.1}$ScO$_{3-\delta}$ at 800 and 900 ˚C.

Composition	600 ˚C	700 ˚C	800 ˚C	900 ˚C	1000 ˚C
BaNdScO$_4$	0.92	0.88	0.76	0.76	0.69
BaNd$_{0.8}$Ca$_{0.2}$ScO$_{3.9}$	0.53	0.62	0.61	0.61	0.51
La$_{0.9}$Sr$_{0.1}$ScO$_{3-\delta}$	0.96	0.85	0.63	0.36	–

(G) TG-MS data and water content y of $BaNd_{0.8}Ca_{0.2}ScO_{3.9} \cdot y\ H_2O$
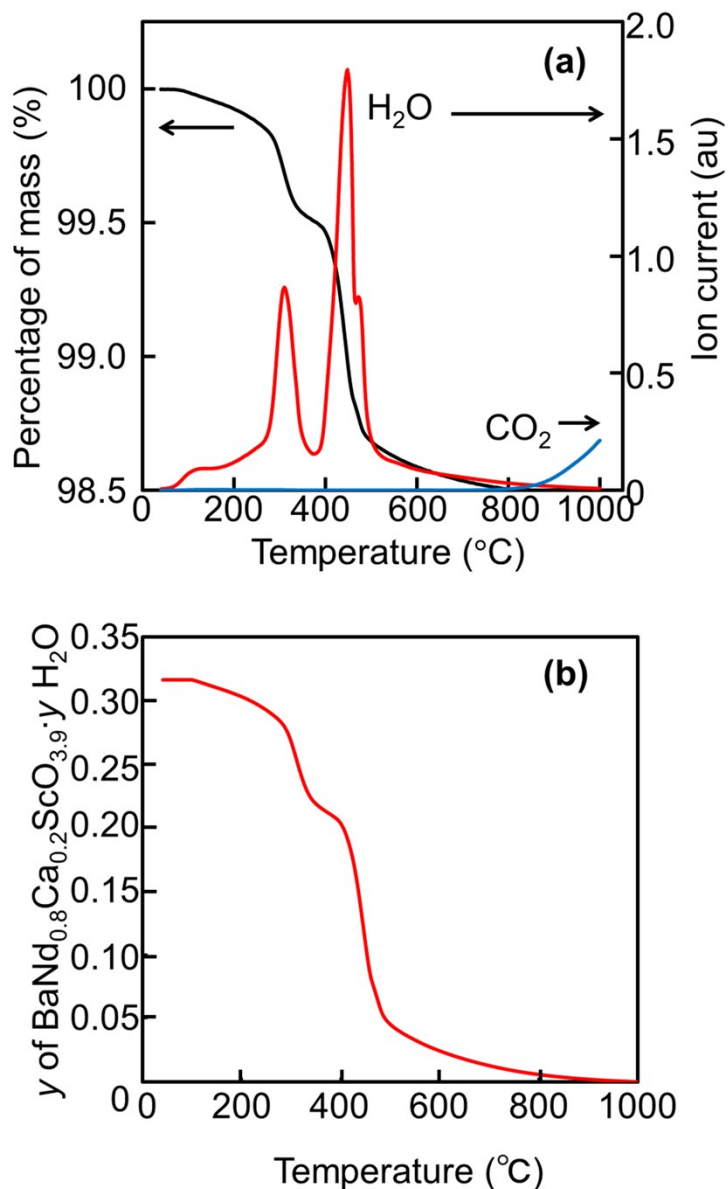
Figure S7. (a) Thermogravimetric-mass spectroscopy (TG-MS) curves of $BaNd_{0.8}Ca_{0.2}ScO_{3.9}$ sample annealed in wet air $[BaNd_{0.8}Ca_{0.2}ScO_{3.934(2)}H_{0.067(3)} \cdot 0.283\ H_2O]$. Black TG curve and ion currents of H_2O (red) and CO_2 (blue). (b) Water content y in $BaNd_{0.8}Ca_{0.2}ScO_{3.9} \cdot y\ H_2O$ obtained using the MS curve.

(H) Results of the structure refinements of $BaNd_{0.8}Ca_{0.2}ScO_{3.9}$ sample annealed in wet air

Table S3. Results of the structure refinements of neutron powder diffraction (NPD) data of $BaNd_{0.8}Ca_{0.2}ScO_{3.9}$ sample annealed in wet air [$BaNd_{0.8}Ca_{0.2}ScO_{3.934(2)}H_{0.067(3)}$·0.283 H_2O] based on eighteen structural models where the positions of H atom are different from each other. For the structure refinements based on the Models 2-18, the atomic coordinates of H atom were fixed. Model 1 gave the best results with lowest R factors. Reliability factors for the structural model without H atom were $R_{wp} = 0.0384$ and $R_F = 0.0264$.

Model No.	Atomic coordinates of H atom			Reliability factors		
	x	y	z	R_{wp}	R_F	R_B
1	0	0.1614(7)	0.8254(17)	0.0381	0.0262	0.0389
2	0.165	0.14	0.615	0.0390	0.0267	0.0411
3	0.88	0.21	0.605	0.0388	0.0266	0.0425
4	0.17	0.14	0.46	0.0393	0.0271	0.0435
5	0.17	0.23	0.46	0.0392	0.0267	0.0449
6	0.17	0.2	−0.1	0.0389	0.0270	0.0421
7	0	0.21	0.18	0.0387	0.0270	0.0394
8	0	0.155	0.75	0.0381	0.0264	0.0392
9	0	0.31	0.25	0.0382	0.0263	0.0400
10	0	0.115	0.52	0.0392	0.0267	0.0438
11	0	0.2	0.65	0.0386	0.0266	0.0414
12	0.35	0.12	0.38	0.0389	0.0269	0.0397
13	0.35	0.09	0.38	0.0393	0.0271	0.0413
14	0.35	0.055	0.38	0.0387	0.0269	0.0386
15	0.26	0.5	0.5	0.0390	0.0271	0.0416
16	0.5	0.56	0.5	0.0387	0.0267	0.0425
17	0.5	0.5	0.32	0.0386	0.0266	0.0411
18	0.5	0.455	0.355	0.0383	0.0265	0.0372

(I) Rietveld pattern of neutron powder diffraction data of BaNd$_{0.8}$Ca$_{0.2}$ScO$_{3.9}$ sample annealed in wet air
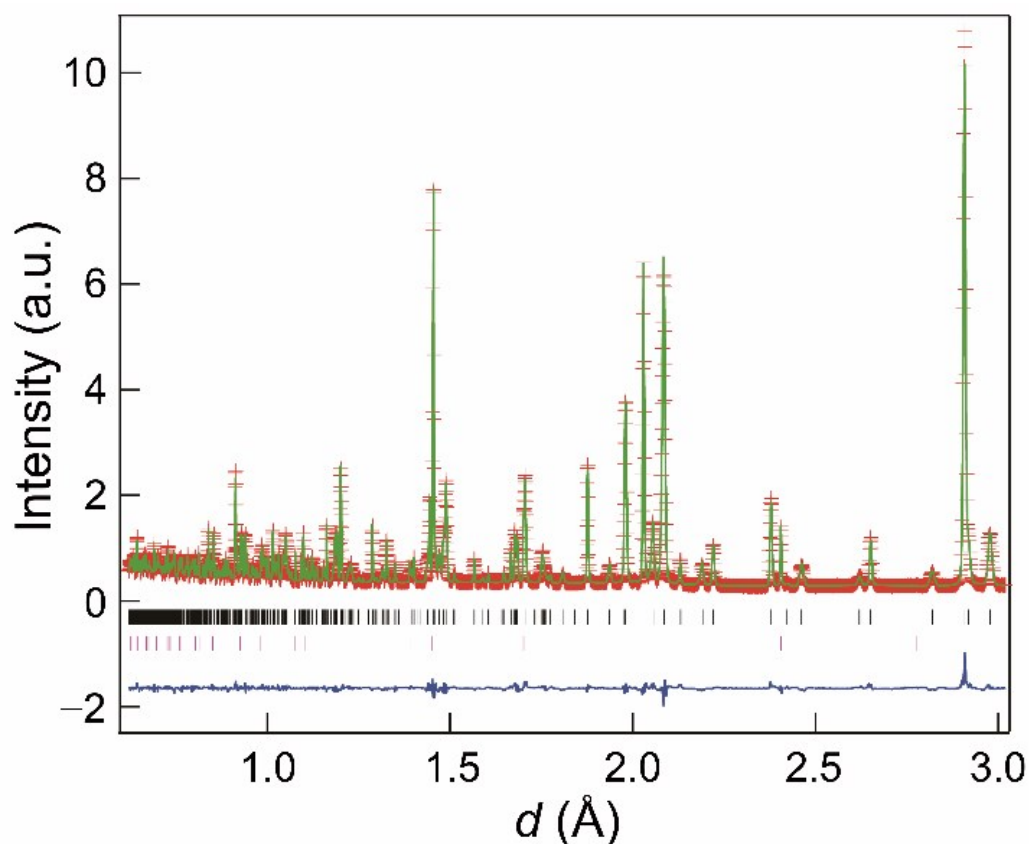
Figure S8. Rietveld pattern of neutron powder diffraction data of BaNd$_{0.8}$Ca$_{0.2}$ScO$_{3.9}$ sample annealed in wet air [BaNd$_{0.8}$Ca$_{0.2}$ScO$_{3.934(2)}$H$_{0.067(3)}$] measured at 25 °C. The observed and calculated intensities and difference plot are shown by red + marks, green solid line, and blue solid line, respectively. Black and purple tick marks stand for the calculated Bragg peak positions of orthorhombic BaNd$_{0.8}$Ca$_{0.2}$ScO$_{3.934(2)}$H$_{0.067(3)}$ and cubic CaO, respectively.

(J) Structural models of $Ba_{20}Nd_{16}Ca_2Sc_{20}O_{80}H_8$ for DFT calculations

Table S4. Energies of $Ba_{20}Nd_{16}Ca_2Sc_{20}O_{80}H_8$ for fifteen structural models, which were obtained by the DFT structural optimizations. Model A−1 is most stable.

| Position of Ca atom*	Structural models	Position of H atom**	Energy (eV)	Energy (meV / atom)
model A	A−1	near O3	0	0
	A−2	near O2	6.872564	47.07236
	A−3	near O1	2.229383	15.26975
model B	B−1	near O3	2.926438	20.04410
	B−2	near O2	8.082557	55.35998
	B−3	near O1	4.192992	28.71912
model C	C−1	near O3	2.171961	14.87645
	C−2	near O2	10.606299	72.64588
	C−3	near O1	5.210950	35.69144
model D	D−1	near O3	2.517771	17.24501
	D−2	near O2	8.868790	60.74514
	D−3	near O1	5.454241	37.35782
model E	E−1	near O3	2.201178	15.07656
	E−2	near O2	8.348209	57.17951
	E−3	near O1	4.713434	32.28379

* In the model A, all Ca atoms occupy the Nd sites. In the models B, C, D and E, all Ca atoms occupy the Ba sites, four Ba atoms are located at Nd sites and the oxygen vacancies exist at different positions depending on the model.

** See the Table 1 for the atom labels and positions of O1, O2 and O3 atoms.

Table S5. Optimized positional parameters of $Ba_{20}Nd_{16}Ca_2Sc_{20}O_{80}H_8$ for the most stable model A−1, which were obtained by the DFT structural optimization (space group $P1$). Optimized lattice parameters a, b, c, α, β and γ are 4.09358 Å, 17.84825 Å, 29.94585 Å, 89.64°, 90° and 90°, respectively. The optimized lattice parameters and average atomic coordinates agree well with experimental ones in Table 1.

atom coordinates	x	y	z		x	y	z		x	y	z		x	y	z
Ba	0	0.4097	0.053	Sc	0	0.0769	0.0483	O1	0.5	0.4929	-0.001	O3	0	0.19	0.5021
Ba	0	0.5609	0.1423	Sc	0	0.9123	0.1458	O1	0.5	0.4926	0.9019	O3	0	0.8187	0.4996
Ba	0.5	0.9181	0.0449	Sc	0.5	0.5707	0.0482	O2	0	0.5832	0.049	O3	0	0.829	0.3952
Ba	0.5	0.0731	0.1401	Sc	0.5	0.3946	0.1452	O2	0	0.4172	0.1511	O3	0	0.1848	0.4079
Ba	0	0.4253	0.2385	Sc	0	0.0776	0.2404	O2	0.5	0.0793	0.0467	O3	0.5	0.6847	0.4929
Ba	0	0.5663	0.3501	Sc	0	0.9341	0.3461	O2	0.5	0.9068	0.1498	O3	0.5	0.3287	0.5052
Ba	0.5	0.916	0.2415	Sc	0.5	0.5797	0.2556	O2	0	0.5973	0.2623	O3	0.5	0.3327	0.5968
Ba	0.5	0.0823	0.3557	Sc	0.5	0.4152	0.35	O2	0	0.409	0.3556	O3	0.5	0.6904	0.3987
Ba	0	0.4272	0.4501	Sc	0	0.0838	0.4524	O2	0.5	0.0953	0.2413	O3	0	0.1846	0.6904
Ba	0	0.5817	0.5445	Sc	0	0.9152	0.5509	O2	0.5	0.9281	0.3501	O3	0	0.8394	0.6923
Ba	0.5	0.9273	0.4507	Sc	0.5	0.584	0.4478	O2	0	0.5931	0.4472	O3	0	0.8076	0.5904
Ba	0.5	0.0664	0.5505	Sc	0.5	0.4334	0.5544	O2	0	0.4274	0.5505	O3	0	0.1865	0.5962
Ba	0	0.4163	0.6587	Sc	0	0.0786	0.6451	O2	0.5	0.0929	0.4535	O3	0.5	0.6889	0.6974
Ba	0	0.5737	0.7595	Sc	0	0.8953	0.7548	O2	0.5	0.9088	0.5452	O3	0.5	0.3156	0.7023
Ba	0.5	0.9244	0.6618	Sc	0.5	0.5773	0.6594	O2	0	0.5947	0.6585	O3	0.5	0.3108	0.7946
Ba	0.5	0.0607	0.7572	Sc	0.5	0.4124	0.7546	O2	0	0.4066	0.7504	O3	0.5	0.6836	0.6046
Ba	0	0.4183	0.8553	Sc	0	0.0711	0.8512	O2	0.5	0.0962	0.639	O3	0	0.1765	0.896
Ba	0	0.5653	0.9507	Sc	0	0.9093	0.949	O2	0.5	0.9172	0.7493	O3	0	0.8043	0.9064
Ba	0.5	0.9101	0.8472	Sc	0.5	0.5772	0.8511	O2	0	0.5796	0.8529	O3	0	0.8275	0.8069
Ba	0.5	0.0651	0.9487	Sc	0.5	0.4093	0.9513	O2	0	0.4024	0.9506	O3	0	0.1775	0.8015
Nd	0	0.7167	0.0498	O1	0	-0.0076	-0.0021	O2	0.5	0.0834	0.851	O3	0.5	0.681	0.8902
Nd	0.5	0.2191	0.0542	O1	0	0.9895	0.097	O2	0.5	0.902	0.9493	O3	0.5	0.3128	0.9021
Nd	0.5	0.774	0.1487	O1	0.5	0.5229	0.2007	O3	0	0.1579	0.1019	O3	0.5	0.305	0.994
Nd	0	0.2781	0.3541	O1	0.5	0.4937	0.0986	O3	0	0.8108	0.1058	O3	0.5	0.6582	0.7972
Nd	0.5	0.2334	0.2445	O1	0	-0.0074	0.1996	O3	0	0.8129	-0.0017	H	0.5	0.6393	0.1913
Nd	0.5	0.797	0.3505	O1	0	0.0263	0.3032	O3	0	0.181	0.0094	H	0.5	0.6698	0.3354
Nd	0	0.7281	0.4457	O1	0.5	0.5	0.4005	O3	0.5	0.6782	0.0984	H	0.5	0.6956	0.7305
Nd	0	0.2963	0.5501	O1	0.5	0.4971	0.3033	O3	0.5	0.3264	0.0938	H	0.5	0.6309	0.5941
Nd	0.5	0.2279	0.4552	O1	0	0.0083	0.4009	O3	0.5	0.3405	0.2085	H	0	0.1397	0.7097
Nd	0.5	0.7782	0.5464	O1	0	-0.0002	0.5001	O3	0.5	0.676	0.0039	H	0	0.169	0.5647
Nd	0	0.7329	0.6563	O1	0.5	0.5251	0.5971	O3	0	0.1838	0.2961	H	0	0.1981	0.1704
Nd	0	0.274	0.7512	O1	0.5	0.5081	0.4995	O3	0	0.8343	0.3036	H	0	0.1303	0.3056
Nd	0	0.7195	0.846	O1	0	-0.0031	0.5973	O3	0	0.8165	0.1981				
Nd	0	0.2676	0.9516	O1	0	0.0197	0.6998	O3	0	0.1907	0.2033				
Nd	0.5	0.2168	0.8506	O1	0.5	0.4896	0.8029	O3	0.5	0.6882	0.304				
Nd	0.5	0.7674	0.9482	O1	0.5	0.4918	0.7003	O3	0.5	0.3078	0.3103				
Ca	0	0.7271	0.2526	O1	0	-0.0056	0.8013	O3	0.5	0.3186	0.401				
Ca	0.5	0.2263	0.648	O1	0	-0.0071	0.9009	O3	0.5	0.6851	0.2098				

(K) Proton diffusion paths and their energy profiles in BaNdScO$_4$H
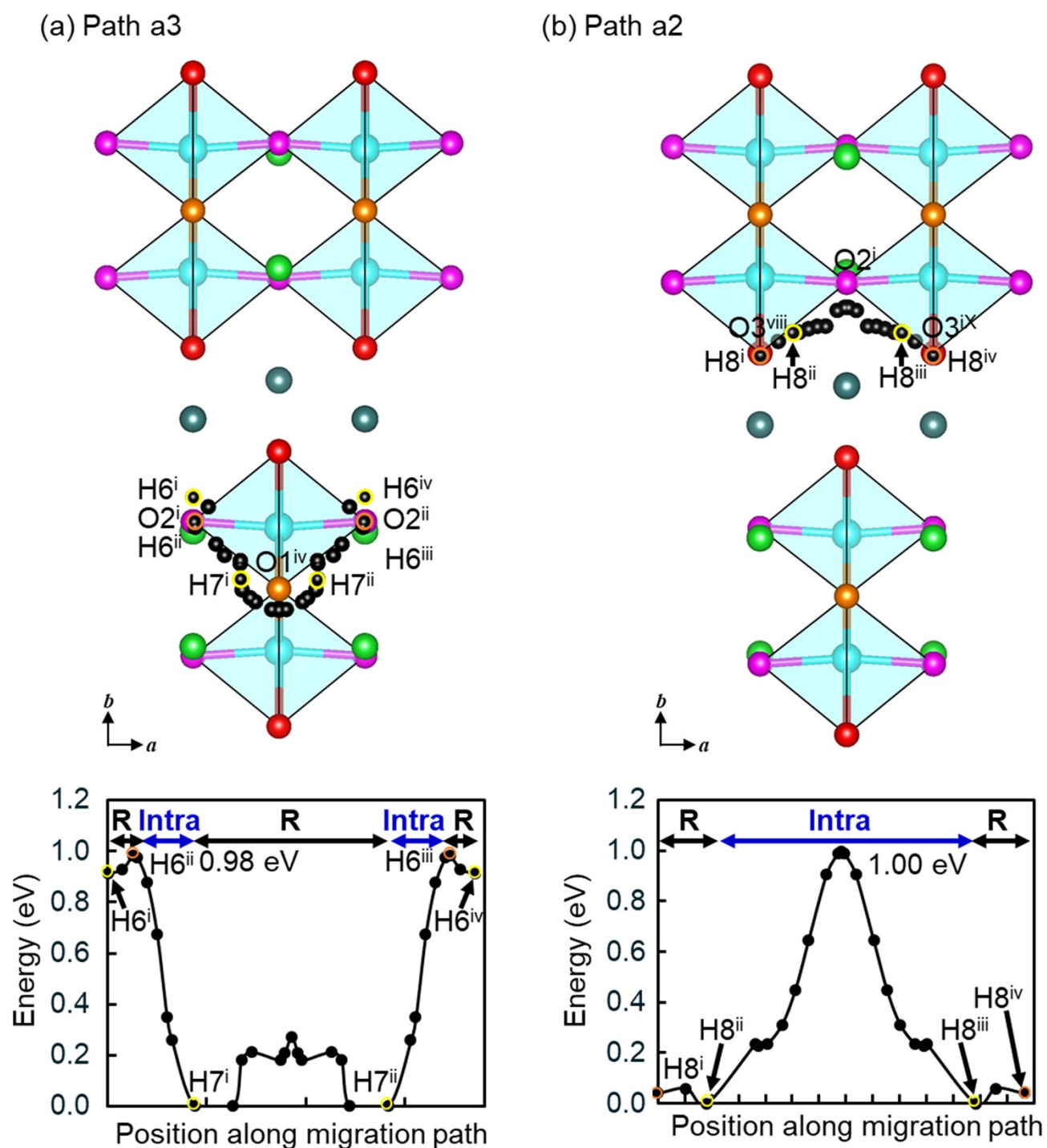
Figure S9. Proton migration pathways and their energy profiles in BaNdScO$_4$H. (a) Path a3 along *a* axis, H6^i(O2^i)–H6^{ii}(O2^i)–H7^i(O1^{iv})–H7^{ii}(O1^{iv})–H6^{iii}(O2^{ii})–H6^{iv}(O2^{ii}) and (b) Path a2 along *a* axis, H8^i(O3^{viii})–H8^{ii}(O3^{viii})–H8^{iii}(O3^{ix})–H8^{iv}(O3^{ix}). See the details in Table 2.

(L) Crystal structures, bond-valence-based energy landscapes and oxide-ion diffusion pathways in BaNd$_{0.8}$Ca$_{0.2}$ScO$_{3.9}$
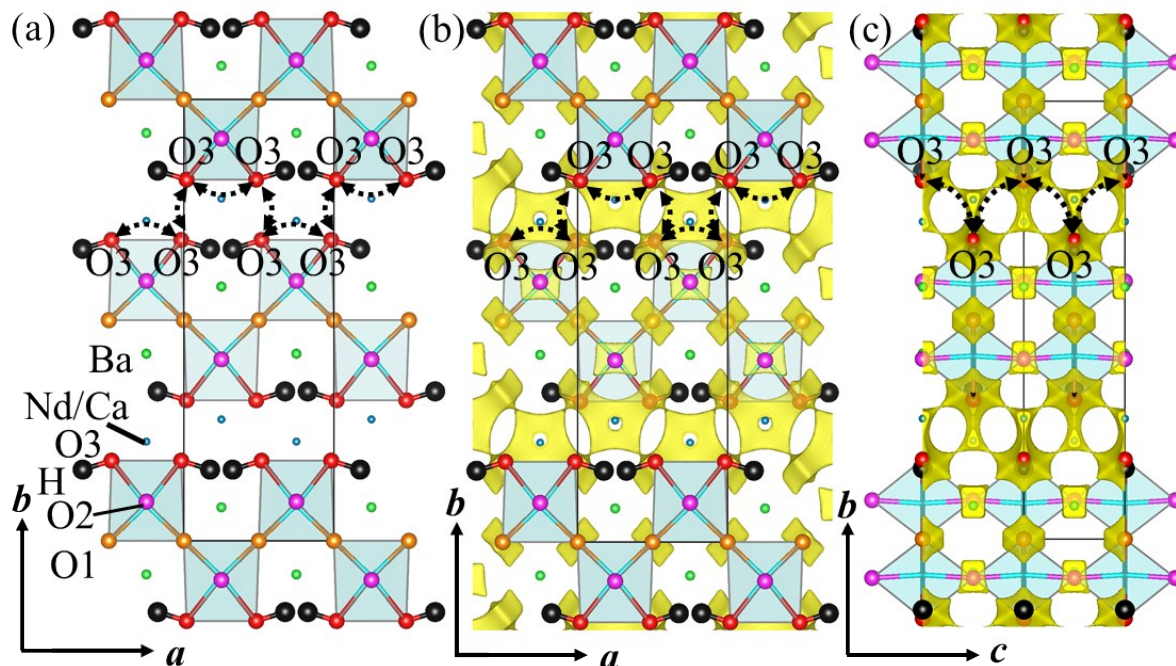
Figure S10. (a) Refined crystal structure and (b,c) bond valence-based energy (BVE) landscapes for an oxide-ion with yellow isosurfaces at 2.00 eV of BaNd$_{0.8}$Ca$_{0.2}$ScO$_{3.934(2)}$H$_{0.067(3)}$ at 25 °C, which were depicted along (a,b) c and (c) a axes. The solid lines represent the unit cell. Orange, pink, red, dark blue, green and black spheres and light blue octahedra stand for O(O1), O(O2), O(O3), Nd/Ca, Ba, H atoms and ScO$_6$ octahedra, respectively. In panels (b) and (c), the most stable position at O3 site was set to 0 eV. Dotted lines with arrows show possible oxide-ion diffusion pathways.

End of Electronic Supplementary Information.